Geoderma 313 (2018) 181–192

Contents lists available at ScienceDirect

Geoderma

journal homepage: www.elsevier.com/locate/geoderma

Impact of multi-day rainfall events on surface roughness and physical crusting of very fine soils

J.E. Bullard[a,*], A. Ockelford[a,c], C.L. Strong[d], H. Aubault[a,b]

[a] Department of Geography, Loughborough University, LE11 3TU, UK
[b] School of Environment, Griffith University, Brisbane, 4111 Queensland, Australia
[c] School of Environment and Technology, University of Brighton, BN2 4GJ, UK
[d] Fenner School for Environment and Society, Australian National University, Canberra, ACT 2601, Australia

ARTICLE INFO

Handling Editor: Yvan Capowiez

Keywords:
Soil surface roughness
Microtopography
Laser scan
Geostatistics
Semivariogram
Disaggregation

ABSTRACT

Soil surface roughness (SSR), a description of the micro-relief of soils, affects the surface storage capacity of soils, influences the threshold flow for wind and water erosion and determines interactions and feedback processes between the terrestrial and atmospheric systems at a range of scales. Rainfall is an important determinant of SSR as it can cause the dislocation, reorientation and packing of soil particles and may result in the formation of physical soil crusts which can, in turn, affect the roughness and hydrological properties of soils. This paper describes an experiment to investigate the impact of a multi-day rainfall event on the SSR and physical crusting of very fine soils with low organic matter content, typical of a semi-arid environment. Changes in SSR are quantified using geostatistically-derived indicators calculated from semivariogram analysis of high resolution laser scans of the soil surface captured at a horizontal resolution of 78 μm (0.078 mm) and a vertical resolution of 12 μm (0.012 mm). Application of 2 mm, 5 mm and 2 mm of rainfall each separated by a 24 h drying period resulted in soils developing a structural two-layered 'sieving' crust characterised by a sandy micro-layer at the surface overlying a thin seal of finer particles. Analysis of the geostatistics and soil characteristics (e.g. texture, surface resistance, infiltration rate) suggests that at this scale of enquiry, and for low rainfall amounts, both the vertical and horizontal components of SSR are determined by raindrop impact rather than aggregate breakdown. This is likely due to the very fine nature of the soils and the low rainfall amounts applied.

1. Introduction

Soil surface roughness (SSR) describes the micro-relief of soils at the centimetre to decimetre scale (Römkens and Wang, 1986). This micro-relief affects the susceptibility of soils to erosion by both water (Kirkby, 2002) and wind (Zobeck and Popham, 1997) through its influence on infiltration (Vidal Vázquez et al., 2006), runoff (Dunkerley, 2004; Helming et al., 1998), overland flow (Darboux et al., 2001; Smith et al., 2011), drainage network evolution (Römkens et al., 2001), evaporation (Allmaras et al., 1977), threshold wind erosion (Chappell et al., 2006) and the surface storage capacity of both water and loose erodible material (Kamphorst et al., 2000; Onstad, 1984). Soil surface roughness also plays a role in modifying exchanges between the terrestrial and atmospheric systems (Rodríguez-Caballero et al., 2012) and affects interactions and feedback processes at a range of scales (Cammeraat, 2002; Smith, 2014).

SSR is controlled primarily by the soil's physical and chemical properties and changes over time in response to both natural and anthropogenically-enhanced physical (erosion/deposition) and biological processes. Römkens and Wang (1986) identified five scales of surface roughness the smallest of which is determined by primary soil particles (≤ mm). The next two scales are driven by the size and organisation of soil aggregates (mm) and by micro-topography (cm) caused by clods and surface cracking. The two largest scales identified are oriented roughness (dm) caused by agricultural activities and topographic roughness (≥ dm) caused by local topography and slope. For those scales where SSR is controlled by soil factors (up to cm scale), the surface roughness of soils typically reduces through time in response to rainfall as the original soil structural units are broken down from macroaggregates (> 250 μm) to microaggregates (20–250 μm) to primary soil particles by slaking, differential swelling, raindrop impacts and physico-chemical dispersion (Emerson and Greenland, 1990; Le Bissonais, 1996a, 1996b). The breakdown of aggregates can result in the formation of physical soil crusts. These crusts typically comprise a thin layer only a few millimetres thick that is more dense and with lower porosity than the underlying soil (Assouline, 2004). Known as

* Corresponding author.
E-mail addresses: j.e.bullard@lboro.ac.uk (J.E. Bullard), a.ockelford@brighton.ac.uk (A. Ockelford), craig.strong@anu.edu.au (C.L. Strong).

http://dx.doi.org/10.1016/j.geoderma.2017.10.038
Received 25 July 2017; Received in revised form 9 October 2017; Accepted 26 October 2017

'seals' when they are wet and crusts when dry, the presence of clays at the surface acts to bind particles together (Shainberg, 1992). Physical crust formation can therefore reduce rates of infiltration and splash erosion, but increase surface runoff and cumulative sediment yield (Agassi et al., 1985; Bradford and Huang, 1993; Kidron, 2007; Morin et al., 1989).

Physical soil crusts can be divided in to those formed by raindrop impact which causes in situ breakdown of aggregates into fine particles (structural crusts) and those formed by the translocation of fine particles into (depositional crusts) or away from (erosional crusts) an area (Shainberg and Letey, 1984; Valentin and Bresson, 1992). Crust formation, and subsequent resistance to erosion, is strongly controlled by soil texture and structure (Bedaiwy, 2007; Hu et al., 2012). For example, Farres (1978) found that soils with large numbers of small aggregates had a greater tendency to structural crust formation than those with fewer but larger aggregates. Crust formation is also affected by the amount, temporal distribution and intensity of rainfall (Fan et al., 2008; Nciizah and Wakindiki, 2014, 2015; Truman et al., 2007). Physical crust formation typically reduces SSR due to the breakdown of aggregates and although the vertical surface change may only be of the order of 1–2 mm, these microrelief dynamics can affect soil erosion processes (Croft et al., 2013; Vermang et al., 2013).

The aim of this research is to determine the impact of rainfall on the surface roughness characteristics and physical crusting of very fine soils. It differs from previous research by focusing only on small aggregates (< 1.4 mm) and therefore only considers the three smallest scales of SSR as identified by Römkens and Wang (1986). The study focuses on dryland soils with very low organic content and on how SSR changes during a multi-day rainfall event typical of a semi-arid region. The specific objectives are to quantify changes in SSR and physical crust strength in response to a multi-day rainfall event, and to investigate whether soil characteristics, such as soil texture or propensity to disaggregation, can explain these changes.

2. Materials and methods

2.1. Sample characteristics

All the soils used in this study were collected from eastern Australia and comprised individual particles and fine aggregates < 1.4 mm diameter (Table 1). Particle-size analysis of the soils was undertaken using a Beckman Coulter LS280 laser sizer in the range 0.375–1000 μm with 85 class intervals. This method of quantifying the particle-size distribution of soils can also lead to the breakdown of soil aggregates. Previous studies have exploited this and used laser sizing to quantify aggregate stability. Following the protocols of Mason et al. (2003, 2011) hydrodynamic disaggregation of the soils was quantified by circulating the samples in a water suspension for 180 min and analysing the particle-size distribution every 1 min for the first 10 min, every 5 min for the next 30 min and every 10 min thereafter. No sonication was used before or during the analysis. In a laser sizer, it is not possible to calculate zero dispersion i.e. no hydrodynamic force applied, and therefore minimal dispersion (MD), the closest measurement to that of the dry soil, is defined as the particle-size distribution measured following 1 min of circulation. The particle-size distribution measured after 180 min of circulation is considered to be mechanically fully-disaggregated and is referred to as the measure of intermediate dispersion (ID). Full disaggregation (FD) which includes sonication and chemical dispersion was not measured in this paper.

For the analyses in this paper, in addition to using the differences in particle-size distribution (clay, silt sand fractions) with minimal and intermediate dispersion as an indicator of aggregate stability, a single indicator was adopted for the purposes of statistical analysis. A number of techniques exist for summarising the aggregate stability of soils using sieve or pipette analyses (e.g. Amezketa, 1999; Le Bissonais, 1996a) but the indicator used here is that known as 'disaggregation reduction' (DR) proposed by Rawlins et al. (2013) who specifically developed it for use where particle size distribution has been determined using laser instruments. Using Rawlins et al. (2013), mean weight diameter (MWD; μm) between continuous size distributions is calculated by:

$$MWD = \sum_{i=1}^{n} \bar{x}_i w_i \quad (1)$$

where $\bar{x}_i$ is the mean diameter of each size fraction (μm), and w_i is the volume proportion (expressed as a decimal proportion) of the sample corresponding to that size fraction. Rawlins et al. (2013) focus on comparing the particle size distribution following complete disaggregation (FD) to the particle-size distribution of water stable aggregates (ID) and therefore they interpret larger values of disaggregation reduction to indicate greater hydrodynamic stability. For this paper, we use the principle of disaggregation reduction to compare MD

Table 1
Locations and characteristics of soil samples. LOI = loss on ignition; Disp. = degree of dispersion; MD = minimal dispersion; ID = intermediate dispersion; DR = disaggregation reduction. See text for details. Crusting Index (CI) is calculated for minimally-dispersed soils.

Sample	Latitude	Longitude	Salinity (μS)	LOI %	Soil type	Disp.	% Clay	% Silt	% Sand	DR (μm)	CI
Diamantina Lakes [c]	− 23.7622	140.9948	101.2	1.06	Sandy loam	MD	6.38	45.19	48.43		1.09
						ID	12.21	39.32	48.48	7.75	
Diamantina Lakes [s]	− 23.7676	140.9951	117.2	0.91	Loamy fine sand	MD	3.85	19.75	76.41		0.87
						ID	12.63	28.96	58.42	12.48	
Spoilbank	− 23.5977	143.2081	38.3	1.66	Sandy loam	MD	3.82	31.33	64.85		0.61
						ID	24.50	45.38	30.12	34.66	
Pimpara Lakes	− 30.4552	141.7019	117.3	1.04	Loamy fine sand	MD	3.42	18.33	78.25		0.76
						ID	14.68	31.07	54.25	61.90	
Eulo	− 28.1422	145.0273	24.5	1.11	Sandy loam	MD	5.18	36.75	58.08		1.17
						ID	11.47	41.85	46.68	10.43	
Thargomindah	− 27.9934	143.8204	23.38	1.01	Silt loam	MD	4.94	50.87	44.19		1.28
						ID	12.22	44.01	43.77	10.24	
Waanaaring	− 29.7006	144.1450	30.1	1.13	Sandy loam	MD	5.43	30.11	64.46		0.82
						ID	12.81	31.83	55.35	10.11	
Mallee Cliffs	− 34.4763	142.4185	139.3	3.16	Sandy loam	MD	7.06	28.65	64.29		0.51
						ID	11.60	36.39	52.01	24.89	
Tapio Station	− 34.0074	142.1507	42.3	1.66	Sandy loam	MD	7.52	26.45	66.03		0.57
						ID	12.25	27.53	60.22	2.87	
Tibooburra	− 29.4291	142.0106	60.7	1.67	Sandy loam	MD	2.91	28.35	68.74		0.68
						ID	22.64	46.89	30.47	26.62	
Lake Millyera	− 31.0363	139.9842	46,700	1.98	Loam	MD	15.71	46.24	38.05		0.21
						ID	58.59	39.83	1.58	48.76	

and ID i.e. disaggregation under hydrodynamic forces only. In this case, smaller values of DR indicate greater hydrodynamic stability.

Soil salinity prior to experimentation was determined using electroconductivity (TPS MC-80 pH-mV-Temp Meter; Rayment and Higginson, 1992) and for ten of the eleven soils sampled ranged from 23 to 140 μS (Table 1). An exceptionally high value of 46,700 μS was obtained for soils from the shore of Lake Millyera which is a highly saline dry lake (Greene et al., 2009). Soil organic matter (SOM) was determined using loss on ignition (Boon et al., 1988). Using these data, the propensity for crusting was summarised using the FAO (1980) Crusting Index (CI). CI is calculated using particle size and soil organic matter content by:

$$CI = \frac{(1.5 \times FineSilt) + (0.75 \times CoarseSilt)}{Clay + (SOM \times 10)} \quad (2)$$

Soils low in clay (%) and in SOM (%) content and high in silt (%) content are highly prone to sealing and crusting. CI $<$ 0.2 indicates no crust formation and a value $>$ 2 is considered a critical limit for high crust formation risk (Moncada et al., 2014). All soils used for these experiments had a 0.2 $<$ CI $<$ 2 suggesting they develop surface crusts (Table 1).

Soils were packed into matte black trays 200 × 140 × 50 mm filled to the surface and lightly compacted. For each soil, three trays were prepared one of which was used for pre-rainfall infiltration measurements and two of which were subjected to rainfall treatments. Of the latter, one tray was used for destructive crust penetration resistance measurements and the other was used for non-destructive measurements (laser profiling) and post-rainfall infiltration. Trays were mounted horizontally beneath the rainfall simulator.

2.2. Rainfall treatments

2.2.1. Multiday rainfall event

There are differences between soil crusts formed during single day rainfall events and those formed during events where rain falls for short periods on consecutive or alternate days (e.g. Bradford et al., 1986; Nciizah and Wakindiki, 2014). Australian Bureau of Meteorology daily rainfall data (2000–2013 inclusive) for 8 meteorological stations in the region from which the soil samples were taken indicate that only 20–35% of rainfall occurs as single events (on one day, with no rainfall on days immediately preceding or following), with the remainder falling during multi-day events with a modal duration of 2 days and a mean duration of up to 2.92 days. The mean number of days on which no rain is recorded between events ranges from 10 to 18 days but can be as long as 193 days suggesting that soils are typically dry prior to rainfall i.e. very low antecedent moisture. Most rainfall events occur during the summer months. Over 76% of rainfall amounts recorded on any one day are $<$ 6 mm. Taking this in to account, the event simulated for all soils tested here was a three day event with a single rain shower of 2 mm on day one, 5 mm on day two and 2 mm on day three, and 24 h drying period between showers. All rainfall was delivered at an intensity of 60 mm h^{-1} (Connolly et al., 1998). Between showers, the soils were dried at 35 °C and 30% humidity to simulate summer conditions in the semi-arid drylands of eastern Australia.

2.2.2. Rainfall simulation

All rainfall experiments were performed using the Griffith University Mobile Rainfall Simulator which is a portable oscillating spray-type rainfall simulator, similar to that described by Loch et al. (2001). A rainfall simulator was used because it makes it possible to control the quantity, intensity and timing of rainfall. The rainfall simulator comprises a water tank with pump and 4× Veejet 80100 nozzles at a height of 2.5 m which sweep across the area of interest at a predetermined rate. Average drop diameter is 3–4 mm. Kinetic energies produced by the nozzles were not measured but previous tests using Veejet 80100 nozzles in a similar type of rainfall simulator have determined values of 29.49 J m^{-2} mm which is similar to that reported for natural rain where intensity exceeds 40 mm h^{-1} (Rosewell, 1986; Loch et al., 2001) Water flow is continuous through the raindrop nozzles and flow not required on the test surface is recycled via catch bins reducing net water consumption at 60 mm h^{-1} to approximately 10 l/min. The wetted area under the rainfall simulator is 2.5 × 1.5 m and the mean Christiansen Uniformity Coefficient (Christiansen, 1942) is 90.23 ± 1.66 which is well above the minimum acceptable value of 80% (Esteves et al., 2000; Iserloh et al., 2013). Rainfall intensity is controlled by altering the rate at which the nozzles sweep across the surface and the wait time at the end of each sweep. To achieve 60 mm h^{-1} rainfall intensity, the sweep duration is 0.55 s and the wait time is 3 s.

Brisbane City Council Mains (BCC) water was used for the experiments. This has a similar pH, but higher concentration of salts than fresh rainwater (Blackburn and McLeod, 1983). Water salinity can affect soil infiltration rate and runoff depth and its impact is affected by soil salinity and texture (Agassi et al., 1994). Salinity in soils decreases aggregate size and increases soil loss by water erosion (Ghadiri et al., 2007) but typically leads to more stable fine aggregates than those formed in less saline conditions (Greene et al., 2006). The electrical conductivity of BCC water was 420 μS cm^{-1} which is substantially higher than natural rainfall inputs recorded in southwest Queensland where values range from 14.13 ± 5.61 μS cm^{-1} to 37.98 ± 23.61 μS cm^{-1} (Biggs, 2006), however experiments focusing on the impact of salinity on soil strength and crust formation suggest the quantities of salts in the water used are not high enough to have a substantial impact on the results obtained here (Kyei-Baffour et al., 2004; Levy et al., 1994).

2.3. Crust measurements

2.3.1. Crust penetration resistance

Soil crust strength was measured using a Geotester pocket penetrometer with a 5 mm diameter tip 24 h after each rainfall simulation. Six measurements of resistance were made after each rain application. Penetrometry is a destructive test and was the only test performed on the soil in these trays to avoid affecting the non-destructive measurements.

2.3.2. Infiltration

Steady state infiltration was determined on dry soils both pre- and post-rainfall simulation. It was measured using a mini-disk infiltrometer (Decagon Devices Inc., 2007) which allows water to infiltrate while under tension to prevent the filling of macropores. Suction rate was varied according to soil type, using higher suction levels for sandy soils and lower suction levels for clay soils, and infiltration rate was determined according to the manufacturer's guidance (Nciizah and Wakindiki, 2014).

2.4. Soil surface roughness characterization

SSR can be measured using contact techniques (e.g. profile or pin meters; Garcia Moreno et al., 2010) but these are not ideal if repeat measurements to examine SSR dynamics are required. Non-contact techniques can enable measurement of surfaces without affecting the surface and include laser scanning (Carmi and Berliner, 2008; Huang and Bradford, 1990, 1992; Vermang et al., 2015a, 2015b) and close-range digital photogrammetry (Brasington and Smart, 2003). Existing studies of small-scale SSR using laser scans typically have a horizontal resolution of ≈ 1–20 mm and a vertical resolution of 0.02–1 mm (e.g. Darboux et al., 2001; Carmi and Berliner, 2008; Sun et al., 2009; Vermang et al., 2013). Given the small-sized aggregates typical of the soils used here it was considered necessary to capture data at a very high resolution so laser scanning at $<$ 0.1 mm horizontal and $<$ 0.02 mm vertical resolution was used.

2.4.1. Laser profiling

To obtain high resolution measurements of soil surface roughness for each sample, the soil surface was scanned using a ScanCONTROL 2900 laser profiler mounted on a computer-controlled, motor-driven traversing frame. The scanner was mounted at a height of 24 cm above the soil surface and used to scan the soil at a horizontal resolution of 78 μm (0.078 mm) and a vertical resolution of 12 μm (0.012 mm). The soil surface was scanned before the rainfall, and after each daily rain application to enable changes in soil microtopography to be determined. Markers were used at the tray edges to ensure that repeat scans could be aligned and the use of matt black trays reduced errors associated with reflection from the tray edges. Having aligned the scans, a central area of 80 × 80 mm in the centre of each scan was extracted for analysis (c. 1.5 million data points). Using data from only the centre of the tray minimises edge effects and the very high resolution makes it possible to identify any small scale impacts of soil aggregate breakdown that lead to changes in soil surface roughness.

2.4.2. Indices of soil roughness and spatial variability

The laser scan data were post-processed by linear interpolation onto a 0.078 mm grid using MatLab to produce digital elevation models (DEMs) of the soil surface before and after each rain application (t = 0; t = 2; t = 7; t = 9 – where the value represents both the total cumulative rainfall amount (mm) and duration in minutes). On a few occasions the laser beam was sometimes occluded returning no data for a given point (< 0.01% of scan data). These null data points were returned as "NaN" values and were replaced by an average value calculated from the surrounding 8 cells. Although our experiments were conducted in controlled laboratory conditions it proved difficult to produce a perfectly smooth soil surface yet any slight gradient of the soil surface has a substantial effect on the scan introducing a slope trend. Consequently, all the z-data were detrended using a linear model to remove any large scale oriented roughness which may create bias in the metrics derived from them. The mean z value for t = 0 was used as the zero level for all digital elevation plots to make it possible to compare the surface after each rain application with the initial conditions.

From the DEM data, a number of aspatial and spatially-resolved indices were used to characterise the soil surface roughness. Aspatial metrics look at bulk properties of the soil surface and include topographic range and random roughness. The topographic range (TR) of each soil scan indicates the difference in height (mm) between the lowest and highest detected points in the DEM. The random roughness (RR), calculated using Eq. (3), is the standard deviation in height after eliminating oriented roughness such as slope (Allmaras et al., 1966; Currence and Lovely, 1970).

$$RR = \sqrt{\frac{1}{n}} \sum_{i=1}^{k} (Zi - \overline{Z})^2 \quad (3)$$

In Eq. (3), Zi is the height reading at location i and k is the number of height readings (Kuipers, 1957).

More recently researchers have taken the spatial complexity of SSR in to account using fractal analyses. Variational techniques (e.g. semivariogram interpretation, root mean square method) are thought to provide a better description of SSR than non-variational techniques (e.g. tortuosity) and have become the most widely used fractal descriptors of soil surfaces (Garcia Moreno et al., 2010; Croft et al., 2013). In this study, for each scan, a semivariogram was produced to which a spherical model was fitted according to Eq. (4) (Corwin et al., 2006) and which was chosen due its known suitability for describing data sets with high short range variability, linear behaviour close to the origin, and where an asymptote (sill) is reached at small ranges.

$$\gamma(h) = c_1 \left[1.5\frac{h}{a} - 0.5\left(\frac{h}{a}\right)^3 \right] + c_0 \quad (4)$$

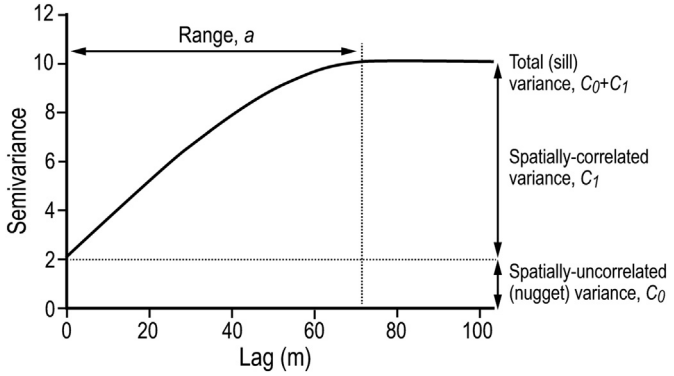

Fig. 1. Generalized semivariogram and key features.
Source: Anderson and Kuhn (2008).

In Eq. (4) γ is semivariance for a given lag distance h. Model results were used to determine four key geostatistically-derived indicators; range (a), spatially-correlated variance (c_1), nugget variance (c_0) and total (sill) variance ($c_0 + c_1$). Each of these values relates to a curve as shown in Fig. 1 and each describes an attribute of SSR. The range (a) indicates the maximum scale of spatial variation in the data (Atkinson and Tate, 2000) such that larger values of a are associated with larger scales of spatial patterning; the value reflects a change in gradient of the curve and is read from the abscissa taking the same units. Nugget variance (c_0) is spatially uncorrelated variance due to factors such as measurement error or model fitting. Sill variance describes the total amount of spatial variation in the data such that, for the same scale, more spatially varied surfaces have higher values of $c_0 + c_1$.

For the soils tested here, there is a strong relationship between sill variance and random roughness (Fig. 2, $R^2 = 0.945$, $p < 0.001$) which highlights the link between the vertical component of roughness and the total amount of spatial variation in the data set (Croft et al., 2013). This should enable any decrease in SSR over time caused by the breakdown of soil aggregates under raindrop impact to be quantified using sill variance (Anderson and Kuhn, 2008; Croft et al., 2009). The other indicator of aggregate breakdown that can be obtained from the semivariogram analysis is the range a. An increase in a occurs as aggregates are compacted in to a spatially continuous layer (Croft et al., 2013). Previous studies have indicated that changes in vertical and horizontal SSR are caused by aggregate breakdown, which can lead to physical crust formation. RR provides a quantitative measure of the vertical component of roughness variation and a provides a quantitative measure of the horizontal component of roughness variation: consequently if aggregate breakdown is the dominant cause of changes in SSR then relationships between RR, a and soil characteristics such as DR and surface resistance might be expected.

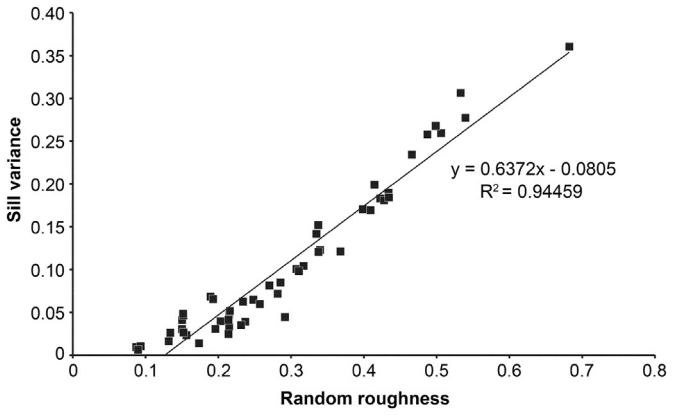

Fig. 2. The relationship between random roughness and sill variance for the sample soils.

Table 2
Summary of SSR and physical crust indicators for different soils. Surface cracking presence (✓) or absence. Time of ponding following start of rainfall is indicated in minutes:seconds. TR = topographic range, RR = random roughness. Variogram statistics a, c_1, c_0, $c_0 + c_1$ extracted from the fitting of a spherical model to the variogram data for each soil after each application of rainfall.

Sample	Cum. rfall (mm)	Cracks	Ponding	Surface Resistance (kg cm^{-2})	Infiltration rate (mm s^{-1})	TR (mm)	RR	Range a (mm)	Spatially-correlated variance c_1	Nugget variance c_0	Sill variance $c_0 + c_1$	RMSE height (μm)
Diamantina Lakes	0			0	0.0059	1.253	0.0873	34.318	0.0075	0.0018	0.0093	0.1871
[c]	2	✓		0.50		5.853	0.3074	3.876	0.0997	0.0010	0.1007	6.0761
	7	✓	3:00	1.58		9.461	0.2034	8.504	0.0273	0.0124	0.0397	2.2000
	9	✓		2.30	0.0008	6.104	0.2340	5.780	0.0622	0.0004	0.0626	0.6658
Diamantina Lakes	0			0	0.1377	2.350	0.1562	28.445	0.0161	0.0072	0.0233	0.6658
[s]	2	✓		0.47		4.703	0.4225	4.223	0.1754	0.0075	0.1829	6.1114
	7	✓	2:00	0.78		4.642	0.2481	9.573	0.0601	0.0047	0.0648	1.4074
	9	✓		0.92	0.0063	4.932	0.3987	5.283	0.1690	0.0016	0.1706	4.2932
Spoilbank	0			0	0.0161	2.932	0.2149	27.739	0.0149	0.0181	0.0330	2.9996
	2	✓		0.20		9.037	0.5062	3.831	0.2413	0.0179	0.2592	15.6856
	7	✓	3:00	0.63		14.978	0.8154	7.479	1.0564	0.0391	1.0955	58.1594
	9	✓		1.00	0.0022	14.900	0.9338	5.755	1.1062	0.00004	1.1062	30.2121
Pimpara Lakes	0			0	0.0178	1.868	0.1893	43.692	0.0684	0.0000	0.0684	2.7000
	2	✓		0.40		5.123	0.4091	4.674	0.1576	0.0117	0.1693	2.2000
	7	✓	4:30	0.68		6.499	0.4146	6.376	0.1991	0.0000	0.1991	10.900
	9	✓		1.12	0.0067	5.221	0.4660	5.181	0.2276	0.0066	0.2342	10.800
Eulo	0			0	0.0235	2.217	0.1503	51.431	0.0409	0.0000	0.0409	0.6829
	2			0.45		5.037	0.3399	4.204	0.1195	0.0035	0.1230	5.4988
	7	✓	3:30	1.07		5.958	0.1959	20.327	0.0144	0.0164	0.0308	2.2094
	9	✓		2.15	0.0042	6.185	0.2572	10.246	0.0432	0.0166	0.0598	4.7273
Thargomindah	0			0	0.0435	1.873	0.1340	39.022	0.0242	0.0021	0.0263	0.2984
	2	✓		0.38		3.773	0.3172	4.265	0.1023	0.0019	0.1042	4.8014
	7	✓	3:45	1.07		6.037	0.2371	17.805	0.0111	0.0279	0.0390	4.5166
	9	✓		2.00	0.0042	3.852	0.2149	6.433	0.0442	0.0030	0.0472	2.5010
Waanaaring	0			0	0.0123	1.530	0.0933	32.147	0.0091	0.0014	0.0105	0.2796
	2	✓		0.50		3.522	0.3378	4.199	0.1164	0.0042	0.1206	6.1000
	7	✓	3:30	0.88		7.850	0.2313	17.163	0.0032	0.0320	0.0352	4.2000
	9	✓		1.70	0.0030	7.987	0.2855	7.864	0.0715	0.0134	0.0849	13.400
Mallee Cliffs	0			0	0.0215	1.730	0.0897	11.927	0.0044	0.002	0.0064	0.6041
	2			0.37		3.895	0.3106	3.764	0.0947	0.0035	0.0982	2.0636
	7	✓	3:00	1.07		9.046	0.2915	30.965	−0.0169	0.0615	0.0446	9.8815
	9	✓		1.83	0.0007	6.760	0.3348	5.812	0.1400	0.0017	0.1417	6.1315
Tapio Station	0			0	0.0357	1.706	0.1928	45.810	0.0653	0.0000	0.0653	1.1000
	2			0.69		4.047	0.3678	7.539	0.0933	0.0278	0.1211	12.500
	7	✓	2:30	0.67		6.422	0.2701	49.045	−0.2317	0.3130	0.0813	3.2000
	9	✓		0.58	0.0028	4.112	0.2815	11.953	0.0535	0.0183	0.0718	7.6000
Tibooburra	0			0	0.0724	1.853	0.1502	22.309	0.0290	0.0014	0.0304	0.9123
	2	✓		0		5.455	0.4343	5.830	0.1621	0.0222	0.1843	11.400
	7	✓		0.02		6.139	0.4987	5.532	0.2628	0.0050	0.2678	11.200
	9	✓		0.3	0.0043	6.607	0.4874	5.517	0.2534	0.0044	0.2578	10.100
Lake Millyera	0			0	No data	3.743	0.3373	35.727	0.1291	0.0229	0.152	4.7000
	2	✓		0.18		7.589	0.6824	16.785	0.1815	0.1789	0.3604	22.100
	7	✓	3:15	0.07		6.349	0.5331	34.504	0.2409	0.0654	0.3063	15.300
	9	✓		0.3	No data	6.346	0.5395	29.836	0.1647	0.1124	0.2771	18.400

3. Results

SSR is visualised using DEMs of the soils before and after rainfall applications, and quantified using topographic range (TR) and features calculated using the empirical semivariograms (Fig. 1). SSR is affected by raindrop impact, which can cause dislocation and re-orientation of surface grains in turn leading to surface ponding if a seal forms, and cracking due to non-uniform shrinkage when the soil dries (Scherer, 1990). All except two of the soils developed superficial cracks after they had dried following 2 mm of rainfall and all dried with deeper cracks following a further 5 mm rainfall (indicated by increases in TR; Table 2). In some cases, the final 2 mm application of rainfall caused some cracks to become less apparent. No ponding occurred on any of the soils during the 2 mm rainfall applications, but ponding did occur on all soils during the 5 mm rainfall, with the exception of that from Tibooburra (Table 2).

Using the nomenclature of Casenave and Valentin (1992), rainfall on the clay-rich, sand-poor soils from Lake Millyera caused a type 1 structural crust to form, comprising a rough surface made of coalescing partially slaked aggregates. This type of crust is generally low strength which is reflected in the low values of surface resistance (0.3 kg cm^{-2}) measured at t = 9 (Table 2). All the other crusts formed in this experiment can be classified as two-layered structural crusts, characterised by a sandy micro-layer at the surface overlying a thin seal of finer particles (type 2 of Casenave and Valentin, 1992) (Fig. 3). These are also known as 'sieving' crusts (Rajot et al., 2003) and are typically of moderate strength and porosity. The thickness of the sandy layer was not measured, but was best developed on soils from Diamantina Lakes [s], Pimpara Lakes, Eulo, Wanaaring, Mallee Cliffs and Tapio Station i.e. those with a high proportion of sand$_{ID}$ (> 49%). The sandy micro-layer formed on the soils is not continuous but is patterned.

3.1. Response of SSR and crusting to a multi-day rainfall event

The impact of rainfall on the SSR of the eleven soils is summarised in Table 2. As all the soils were smoothed and packed prior to the application of rainfall, values of TR and RR are lowest for t = 0. For all soils the application of 2 mm rainfall (t = 2) resulted in a substantial increase in RR and a decrease in a. These changes reflect a change from large scale patterning (high a) associated with a smooth surface (low

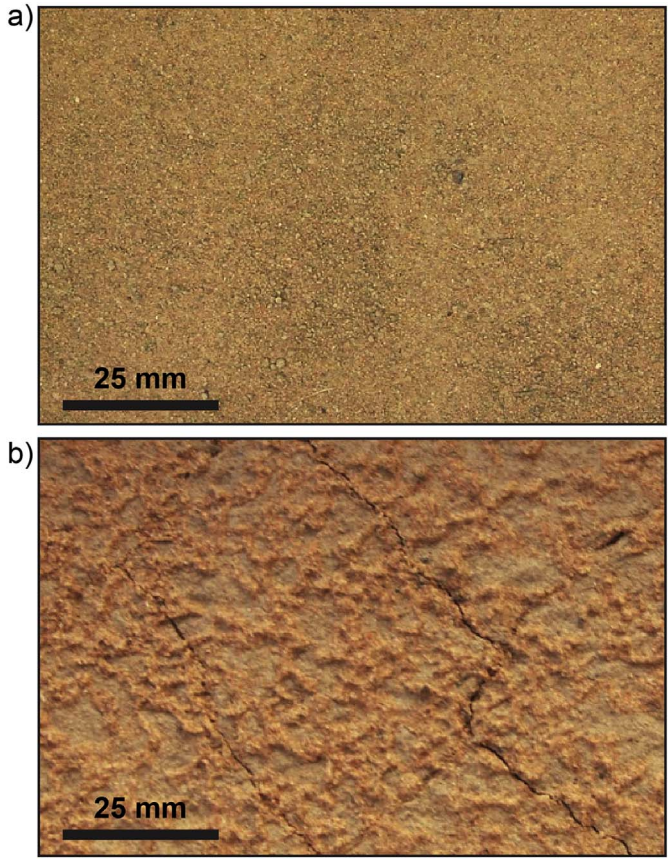

Fig. 3. Soils from Diamantina Lakes [s] (a) dry soil, t = 0; (b) following a multi-day rainfall event at t = 9. The soil in (b) clearly shows the development of a two-layered structural crust with a layer of fine sands overlying a thin seal of finer particles.

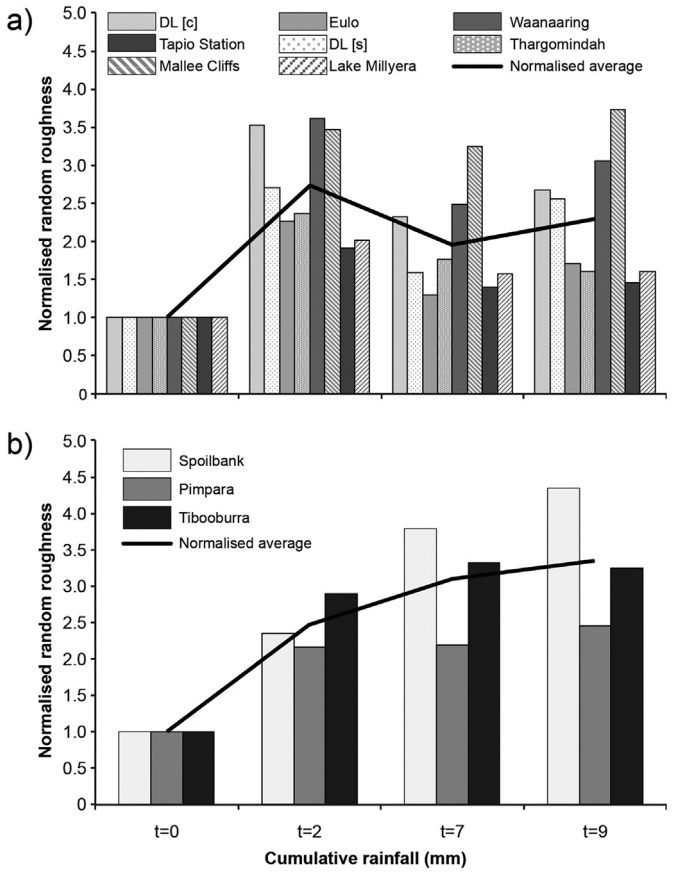

Fig. 4. Changes in RR with cumulative rainfall normalised to RR at t = 0 for (a) soils where RR is higher for t = 2 and t = 9 compared with t = 0 and t = 7 and (b) soils where RR increases or shows minimal change through time. DL = Diamantina Lakes.

RR) to a rough surface with small scale patterning. Further rainfall (t = 7) leads to a decrease in RR for the majority of the soils as the surface becomes smoother and less patterned, possibly in response to surface ponding followed by a slight increase at t = 9 in response to the final 2 mm application of rain (Fig. 4). Three soils behave slightly differently (Spoilbank, Pimpara Lakes, Tibooburra) in that RR does not decrease after the 5 mm rainfall (t = 7) and remains high throughout the remainder of the experiment. With the exception of Tibooburra (which remains constant) all soils have a higher a at t = 7 compared with t = 2 or t = 9 suggesting larger scale patterning after the 5 mm compared with after the 2 mm rainfall application (Table 2). The extent of the increase at t = 7 is very variable cross the soils. For Diamantina Lakes ([c] and [s]), Spoilbank, and Pimpara Lakes the increase in a is < 6 mm, for all other soils the increase is much higher and in the range 13–40 mm.

Figs. 5 and 6 illustrate how two of the soils responded to rainfall. For Tapio Station (Fig. 5), the first 2 mm of rainfall caused the development of a sieving crust at the soil surface with clear small scale raindrop patterning visible in the photograph and DEM and characterised by a large decrease in a (from 45.81 to 7.539 mm). The addition of 5 mm rainfall led to ponding within 2 min 30 s and the surface became smoother and less patterned (a = 49.045 mm). TR and RR decreased and a increased after the final 2 mm rainfall (t = 9). Typically the semivariogram curves are smooth with no marked periodicity. For the Pimpara Lakes soil, the soil surface became rougher after 2 mm rainfall developing small scale patterns that are visible in the photograph and digital elevation model (Fig. 6). TR and RR increased from 1.868 to 5.123 mm and 0.1893 to 0.4091 respectively (Table 2). The value of a decreased from 43.69 mm (large scale patterning associated with a smooth surface) to 4.67 mm which reflects small scale patterning. When the soil was treated with a further 5 mm of rainfall (t = 7) TR and RR increased further to 6.499 mm and 0.4146 respectively and the scale of spatial patterning increased by ≈2 mm to a = 6.38. The third and final application of rainfall caused a decrease in TR possibly as a result of particle movement infilling the surface cracks but RR increased further. The semivariograms for Pimpara Lakes at t = 7 and t − 9 demonstrate a weak periodicity of the order 10 mm wavelength.

With the exception of soils from Tapio Station and Lake Millyera, the physical crust strength of all soils, as measured using penetrometry, increases with each application of rainfall (Fig. 7). The normalised data indicate that on average crusts formed at t = 7 are twice as resistant and crusts present at t = 9 are 3.5 times as resistant as those formed at t = 2. Infiltration rate on the dry, uncrusted soils ranged from 0.0059 to 0.1377 mm s^{-1} (Table 2). In all cases, the infiltration rate decreased at the end of the 3-day experiment indicating the formation of a physical crust (Table 2). Infiltration on the Pimpara Lakes soils changed the least, by a factor of 2.6 from 0.0178 mm s^{-1} to 0.0067 mm s^{-1} while the greatest change was observed on soils from Mallee Cliffs which reduced by factor of nearly 30 from 0.0215 mm s^{-1} to 0.0007 mm s^{-1}.

3.2. Relationships among SSR, soil characteristics and crusting

The relationships between soil properties for different cumulative rainfall amounts are shown in Table 3. For all rainfall treatments there is a significant positive relationship between topographic roughness (TR) and random roughness (RR) which is to be expected given both capture aspects of microtopography from the DEMs. The initial range of values of TR_0 is very low (TR_0 min 1.235, max 3743) due to the artificial smoothing of the soil surfaces prior to raindrop impact and

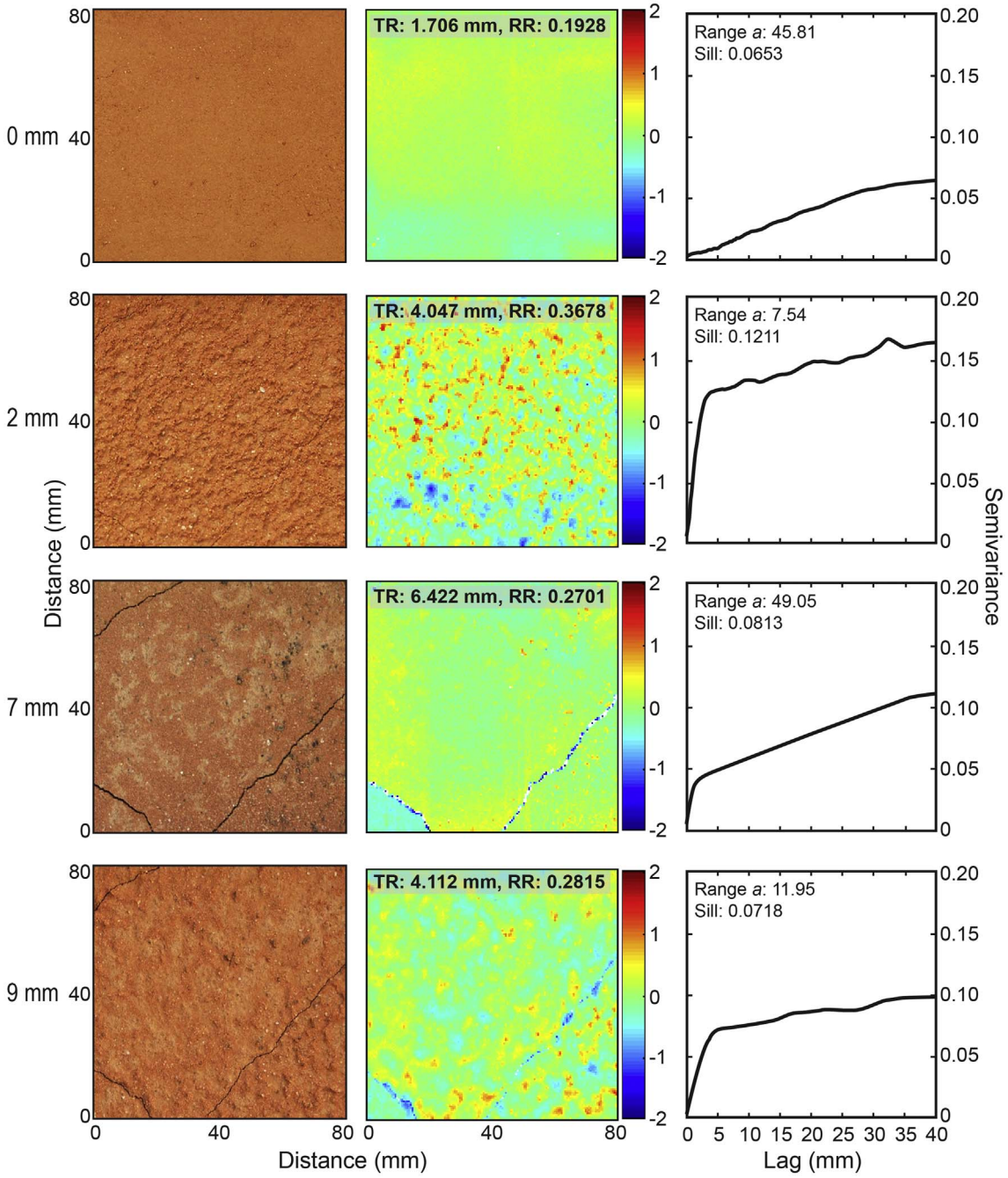

Fig. 5. Changes in SSR after consecutive applications of rainfall on soil from Tapio Station as represented by photographs (left), digital surface models (centre) and empirical semivariograms (right).

although TR_0 and TR_2 are significantly related to the % of $sand_{ID}$ (negative relationship), $silt_{ID}$ and $clay_{ID}$ (positive relationships) in the samples, there is no relationship between TR and any particle size fraction for t = 7 or t = 9. As the amount of rainfall applied increases, TR also increases (TR_2 3.522–9.037 mm; TR_7 4.642–14.978 mm; TR_9 3.852–14.9 mm) due to crack formation. Despite the sustained positive relationship with RR, TR is therefore not considered to be the most suitable parameter for quantifying overall surface roughness at the aggregate scale and below for these soils.

For all rainfall treatments there is a significant negative relationship between $sand_{ID}$ and RR and a positive relationship between RR and $silt_{ID}$ and $clay_{ID}$, but the positive relationships weaken from t = 2 to 7 to 9 i.e. with increased cumulative rainfall through time. These results suggest that soils with a higher proportion of silts and clays are rougher than those containing more sand. DR captures changes due to disaggregation in the whole particle-size distribution of the soil rather than a single descriptor (such as sand, silt, clay), and for all treatments there is a significant positive relationship between RR and DR. This suggests that surfaces with more hydrodynamically-stable aggregates (low DR) are smoother than those with less stable aggregates (high DR). Whilst this might seem counter-intuitive, the soils with less stable aggregates, which contain higher proportions of silt and clay, will rapidly develop sieving crusts where the sand fraction at the surface is the main cause of roughness.

For all rainfall treatments there are negative relationships between surface resistance and each of RR, DR and $clay_{ID}$. This likely reflects the particle size distribution of the soils. Crusts on soils with relatively high clay content were extremely thin and whilst the crusts formed, they

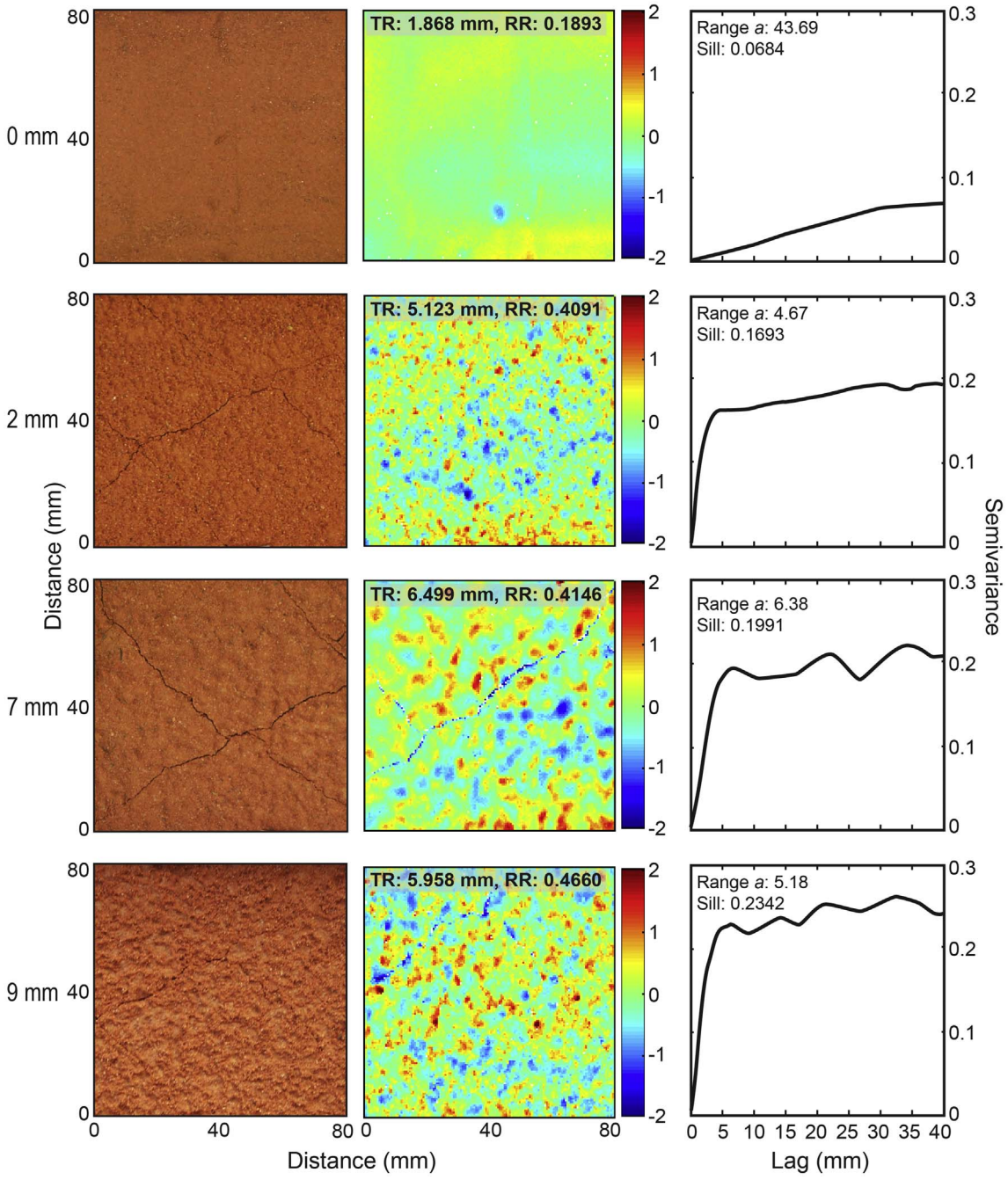

Fig. 6. Changes in SSR after consecutive applications of rainfall on soil from Pimpara Lakes as represented by photographs (left), digital surface models (centre) and empirical semivariograms (right).

were very weak. Previous research suggests that there should be a positive relationship between silt and crust strength because the presence of silts weakens soil structure and aggregates, and results in stronger crusts (Evans and Buol, 1968; Ramos et al., 2003; Bedaiwy, 2008) however relationships between these variables were inconsistent in this study. Overall the crust strength is likely to be determined by the full particle size distribution of the soils, which affects particle packing, and by the fact that less hydrodynamically stable (high DR) soils are more likely to seal rapidly and form a stronger crust.

For all rainfall treatments, there is a significant positive relationship between $clay_{MD}$ and *a*. For t = 2 and t = 9 (2 mm applications) there is a significant positive relationship between $clay_{ID}$ and *a*, and a significant negative relationship between $sand_{ID}$ and *a* (but no relationships for t = 7). This suggests the more clay in the soil, the larger the pattern scale (smoother the surface); more sand is associated with smaller scale patterning. The surface sands in the sieving crusts created here are highly patterned (Fig. 3) for t = 2 and t − 9. For some soils, such as Pimpara Lakes (Fig. 6), the small scale patterning is retained even during the larger rainfall application (t = 7) but for others, such as Tapio Station (Fig. 5) the pattern scale increases (smooths) at t = 7 probably as a result of lateral movements of grains over short distances during ponding.

There is no relationship between dry soil infiltration rates (Inf_0) and any other variable. However at the end of the experiment, soils with higher clay content ($clay_{MD}$) had lower rates of infiltration than those with a higher sand content ($sand_{MD}$). Previous research has found that there is a relationship between aggregate stability (DR) and organic matter content (LOI%) even for soils with very low organic content (e.g.

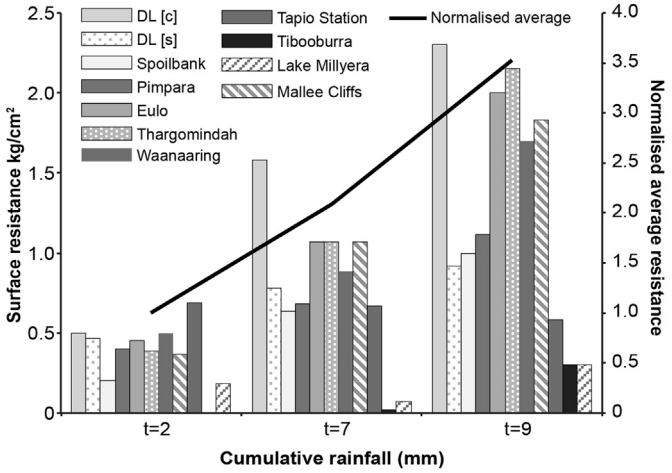

Fig. 7. Soil surface resistance for all soils with cumulative rainfall from t = 2 to t = 9. Mean indicates the normalised average change in resistance. DL = Diamantina Lakes.

1–2% REFS) but that is not supported by this study, possibly due to the very fine nature of the aggregates. There is no significant relationship between salinity and DR. The statistical analysis excludes the soil from Lake Millyera which has extremely high salinity (46,700 μS). Other descriptors for Lake Millyera are of the same order of magnitude as other soils in the data set which suggests that in this instance, the high salinity is not leading to substantially different behaviour compared with less saline soils.

4. Discussion

In accordance with previous studies, physical crust strength has been found to increase with cumulative rainfall (Fan et al., 2008; Feng et al., 2013; Freebairn et al., 1991; Nciizah and Wakindiki, 2014). However, some of the relationships between rainfall and SSR determined here differ from those identified in other research. Studies examining the impact of rainfall on soil surface roughness for coarser soil aggregates (typically > 2 mm) and at a lower spatial resolution than used here, suggest that with increased rainfall, values of TR increase and RR decrease (Jester and Klik, 2005; Carmi and Berliner, 2008; Vermang et al., 2015a, 2015b; Anderson and Kuhn, 2008; Croft et al., 2009). In this study, TR for all rainfall treatments is higher than for dry soils, but there is no systematic increase with cumulative rainfall. For six of the soils TR is highest at t = 7, for four soils TR is highest at t = 9. As TR reflects the minimum and maximum values on the DEM it can capture low values associated with the opening up of cracks in the soil surface. Photographs and DEMs of the soil surfaces suggest that on some soils the final 2 mm of rainfall triggered a widening and deepening of cracks whilst on other soils it caused the cracks to infill with

Table 3
Pearson correlation coefficients (r) between variables for (a) t = 0; (b) t = 2; (c) t = 7; (d) t = 9. Subscript 0, 2, 7, 9 indicates cumulative rainfall after which the variable was measured. Subscript MD and ID indicate minimal and intermediate dispersion respectively. Bold values of r indicate statistically significant at 0.1 probability level (two-tailed), bold* indicates significant at 0.05 probability level (two-tailed). There are no penetrometer (Pen) measurements for t = 0. Infiltration rates (Inf) were only measured for t = 0 and t = 9. Correlations for salinity exclude Lake Millyera.

(a)

t = 0	TR_0	RR_0	a_0	Inf_0	DR
TR_0	1				
RR_0	**0.8852***	1			
a_0	0.0263	0.2632	1		
Inf_0	0.2966	0.1663	− 0.2042	1	
DR	**0.5138**	**0.5877**	− 0.0845	− 0.1577	1
$Sand_{MD}$	− 0.3374	− 0.2954	− 0.1504	0.3750	0.1143
$Silt_{MD}$	0.3014	0.2463	0.1548	− 0.3566	− 0.1452
$Clay_{MD}$	0.4918	**0.5474**	0.0831	− 0.3981	0.1209
$Sand_{ID}$	**− 0.8096***	**− 0.7671***	0.0674	0.0504	− 0.4987
$Silt_{ID}$	**0.6699***	**0.5341**	− 0.2289	− 0.1542	0.4160
$Clay_{ID}$	**0.8415**	**0.8702***	− 0.0174	0.1562	**0.5434**
LOI%	0.1743	0.0906	− 0.6319	− 0.1991	0.2063
Salinity	− 0.1981	− 0.2339	− 0.4838	0.2180	0.3961
CI	− 0.1541	− 0.2148	0.4328	0.0361	− 0.2173

(b)

t = 2	TR_2	RR_2	a_2	Pen_2
TR_2	1			
RR_2	**0.7371***	1		
a_2	0.3702	**0.8135***	1	
Pen_2	**− 0.5552**	**− 0.5584**	**− 0.6574***	1
DR	0.5046	**0.6296***	0.3923	**− 0.5426**
$Sand_{MD}$	− 0.2259	− 0.2639	**− 0.5617**	0.0834
$Silt_{MD}$	0.2237	0.2173	0.4963	− 0.0963
$Clay_{MD}$	0.1828	0.5078	**0.8529***	0.0247
$Sand_{ID}$	**− 0.7519***	**− 0.8683***	**− 0.7642***	**0.7286***
$Silt_{ID}$	**0.7633***	**0.6734**	0.5018	**− 0.8366***
$Clay_{ID}$	**0.6087***	**0.9328***	**0.9327***	**− 0.5417***
LOI%	0.0790	0.1569	0.2423	− 0.2795
Salinity	− 0.0764	− 0.0549	− 0.2392	0.00568
CI	0.0595	− 0.2190	− 0.3327	− 0.0109

(*continued on next page*)

Table 3 (*continued*)

(c)

t = 7	TR_7	RR_7	a_7	Pen_7
TR_7	1			
RR_7	**0.6177***	1		
a_7	−0.2049	−0.2150	1	
Pen_7	−0.0307	**−0.5328**	−0.1523	1
DR	0.1350	**0.6331***	−0.2176	−0.4137
$Sand_{MD}$	−0.0109	0.0722	−0.3397	**−0.7671***
$Silt_{MD}$	0.0315	−0.0773	0.2762	**0.7567***
$Clay_{MD}$	−0.1292	−0.0193	**0.6742**	0.5074
$Sand_{ID}$	−0.1603	**−0.6544***	−0.0062	0.0181
$Silt_{ID}$	0.3534	**0.6841***	−0.1570	0.1988
$Clay_{ID}$	−0.0287	**0.5327**	0.2377	**−0.6052***
LOI%	0.2832	0.2632	0.4836	−0.0280
Salinity	−0.0699	−0.0949	−0.1493	0.1514
CI	−0.0722	−0.1753	**−0.6462***	0.3700

(d)

t = 9	TR_9	RR_9	a_9	Pen_9	Inf_9
TR_9	1				
RR_9	**0.8181***	1			
a_9	−0.1019	0.0960	1		
Pen_9	−0.0926	**−0.5344**	−0.4318	1	
Inf_9	−0.3606	0.0202	−0.1239	−0.3786	1
DR	0.2380	**0.5914**	0.2871	−0.4353	0.3725
$Sand_{MD}$	0.1128	0.1927	**−0.6516***	−0.2248	**0.5533**
$Silt_{MD}$	−0.0975	−0.1974	**0.5876**	0.2755	−0.5181
$Clay_{MD}$	−0.1860	−0.1109	**0.9099***	−0.1713	**−0.6766***
$Sand_{ID}$	−0.3319	**−0.5468**	**−0.7234***	0.4882	0.0757
$Silt_{ID}$	0.4820	**0.5761**	0.4749	−0.2840	−0.2626
$Clay_{ID}$	0.1397	0.4376	**0.8854***	**−0.6085***	0.1497
LOI%	0.1980	0.1994	0.2229	−0.1841	**−0.5830**
Salinity	−0.1977	−0.0170	**−0.5623**	−0.0246	0.0157
CI	−0.0390	−0.1565	−0.2871	0.4429	0.3173

detached soil particles. Croft et al. (2013) found that where networks of cracks form on soil surfaces, these are reflected as periodic oscillations in the semivariogram in which lag distances are related to crack polygon diameters. Where cracks are larger or not repeated within the observational area, as is the case for all soils in this study, the semivariogram increases along a steady gradient until maximum semivariance is reached. This means at the scale of analysis used here it is not possible to use the semivariogram to characterise patterns of surface cracking (microtopographic scale).

The response of SSR to raindrop impact can vary as a function of scale and rainfall treatment. For example, using experiments with a rainfall simulator, Huang and Bradford (1992) identified that the response to successive applications of rainfall varied depending on soil surface conditions and processes acting on the surface such that for some soils soil roughness increased, and for others it decreased. In cases where rainfall amount and intensity is insufficient to cause the development of erosional features such as rills, RR typically decreases with rainfall because raindrop impact causes disaggregation and dislodgement of particles. Le Bissonais et al. (1989) found that for < 2 mm rainfall soil aggregate breakdown occurred without displacement of particles, 7 mm rain starts to dislodge microaggregates and wash them in to inter-aggregate spaces in the soil, and the smoothest soil surface develops when ponding causes individual fine particles at the surface to infill pores. Unlike most previous studies, for the soils tested here RR is higher after all applications of rainfall than it is at t = 0, although the increase is not systematic for all sites (Table 2). This suggests that the vertical (RR) component of SSR is not primarily controlled by aggregate breakdown at this scale of inquiry. Croft et al. (2013) suggest that where aggregates dominate surface roughness, the horizontal component of SSR (a) has values similar to the aggregate size range and that as aggregates breakdown, values of a will exceed the maximum sieved size range. For this study, maximum aggregate size is 1.4 mm. All values of a for all soils exceed this value, including those for dry soils. If a is linked to aggregate breakdown then values of a should initially be associated with aggregate size and then increase as aggregate breakdown takes place. For this study, values of a are nearly all at a maximum at t = 0, decrease at t = 2, increase at t = 7 (to different extents) and decrease again at t = 9.

The above suggests that for the fine soils with small aggregates (< 1.4 mm) being tested here, both the vertical (RR) and horizontal (a) components of SSR are being determined by a surface roughness element other than aggregation. Pitmarks on the visible photographs and spatial patterns on the soil DEMs suggest that raindrop impact is the most likely driver of SSR. Compared to many previous studies we are not only focusing on smaller aggregates but, by simulating rainfall events typical of a semi-arid environment, we are also investigating the impact of lower total rainfalls and lower intensities of raindrop impact. Raindrops falling on dry, unconsolidated soils displace sediments both vertically and laterally. A 3–4 mm diameter raindrop, as delivered by the rainfall simulator used here, falling on fine sand (150–200 μm diameter) would be expected to produce a crater 15–20 mm diameter and 0.7–1 mm deep (below the bed surface) with a raised rim around the depression (Furbish et al., 2007; Long et al., 2014; Ryźak et al., 2015). As the rainfall starts to wet the soil surface, the diameter of the impact craters becomes smaller (Ryźak et al., 2015; Zhang et al., 2015). Rain impact detachment of soil particles also reduces as a surface seal forms at the surface (Bradford et al., 1986). This means that although initial raindrop impact craters are quite large and might be expected to

result in higher values of a, during the rainfall event craters may become smaller as the surface becomes reorganised. Results here suggest that for most of the soils the value of a calculated from the semivariogram reflects raindrop impacts because following the first 2 mm application of rainfall the spatial patterning described by a has a length scale in the range 3 to 20 mm, where the low number is typical of merged or coalescing craters and the larger value is typical of distinct and discrete raindrop impact craters.

Raindrop splash particle detachment studies show that less energy is required to detach fine sand particles (100–200 μm) than those which are coarser or finer than this range (Salles et al., 2000), and that splash lengths are also longer for fine sands than other sediments (Leguédois et al., 2005). This suggests silt-rich, less stable aggregates are more likely to be broken apart by raindrop impact (Fu et al., 2017) and compacted to create a seal or crust whilst fine sands that are more likely to be mobilised by rain splash detachment are temporarily entrained and retained on the soil surface, hence forming the sieving crust. The soil surface roughness, as measured here, is therefore dynamic and reflects both the nature of the sediments rearranged by the rainfall event as well as the raindrop impacts. Rajot et al. (2003) suggested that for soils with < 5% clay the development of a sieving crust in response to an initially high rainfall amount (> 40 mm with up to 80 mm h^{-1} intensity) may reduce water erosion but would not reduce wind erosion. This is due to the presence of coarser sand particles on top of the fine clay-dominated crust that could continue to cause sandblasting by saltation. The erosivity of the soils after crusting was not tested for this study, however the reduction in infiltration rates and associated ponding of water at the soil surface suggests the light rain applied is sufficient to affect water erosion processes.

5. Conclusions

The impact of rainfall on the surface roughness characteristics of very fine soils clearly depends upon the quantity rainfall received and also rainfall antecedence. Low quantities of rainfall (2 mm) caused an increase in surface roughness whereas a higher (5 mm) amount of rainfall resulted in a reduction of soil surface roughness for some soils due to ponding. If a surface crust had already formed due to antecedent rainfall, the impact of 2 mm rainfall on soil surface roughness was typically less than when the rain fell on dry, uncrusted soils (comparing t = 2 with t = 9). A type 2 structural sieving crust formed on all the soils examined here and this became stronger (higher surface resistance/strength) and better developed with each subsequent application of rainfall over the 3 day experiment. Changes in SSR were quantified using high resolution laser profiling and semivariogram statistics. Analysis of the semivariogram statistics and soil characteristics clearly revealed that both the vertical (RR) and horizontal (a) components of SSR on very fine soils are primarily controlled by raindrop impact rather than soil particle size or aggregate stability.

Acknowledgements

Many thanks are due to Kyle Barton, Hossein Ghadiri and Grant McTainsh (Griffith University) for assistance with sample preparation and the use of the rainfall simulator. Barry Rawlins and Rachel Efrat (British Geological Survey) provided advice on calculation of DR. JEB, CLS and HA were funded by the UK Natural Environment Research Council (NE/K011461/1); AO was funded by Loughborough University. Soil samples obtained from Diamantina Lakes National Park under permit number: WITK15785115 granted by the Queensland Government, Department of Environment and Heritage Protection. Data used in this paper form part of the NE/K011461/1 dataset archived at the UK National Geoscience Data Centre (http://www.bgs.ac.uk/services/ngdc/home.html release date end 2019).

References

Agassi, M., Morin, J., Shainberg, I., 1985. Effect of drop impact energy and water salinity on filtration rates of sodic soils. Soil Sci. Soc. Am. J. 49, 186–190.
Agassi, M., Shainberg, I., Van der Merwe, D., 1994. Effect of water salinity on inter-rill erosion and infiltration: laboratory study. Aust. J. Soil Res. 32, 595–601.
Allmaras, R.R., Burwell, R.E., Larson, W.E., Holt, R.F., 1966. Total porosity and random roughness of the interrow zone as influenced by tillage. USDA Conserv. Res. Rep. 7, 1–22.
Allmaras, R.R., Hallauer, E.A., Nelson, W.W., Evans, S.D., 1977. Surface energy balance and soil thermal property modifications by tillage induced soil structure. Univ. Minn. Agric. Exp. Station. Tech. Bull. 306, 1–40.
Amezketa, E., 1999. Soil aggregate stability: a review. J. Sustain. Agric. 14, 83–151.
Anderson, K., Kuhn, N.J., 2008. Variations in soil structure and reflectance during a controlled crusting experiment. Int. J. Remote Sens. 29, 3457–3475.
Assouline, S., 2004. Rainfall-induced soil surface sealing: a critical review of observations, conceptual models and solutions. Vadose Zone J. 3, 570–591.
Atkinson, P., Tate, N., 2000. Spatial scale problems and geostatistical solutions: a review. Prof. Geogr. 52, 607–623.
Bedaiwy, M., 2007. Mechanical and hydraulic resistance relations in crust-topped soils. Catena 72, 270–281.
Bedaiwy, M.N.A., 2008. Mechanical and hydraulic resistance relations in crust-topped soils. Catena 72, 270–281.
Biggs, A.J.W., 2006. Rainfall salt accessions in the Queensland Murray-Darling Basin. Aust. J. Soil Res. 44, 637–645.
Blackburn, G., McLeod, S., 1983. Salinity of atmospheric precipitation in the Murray-Darling Drainage Division, Australia. Aust. J. Soil Res. 21, 411–434.
Boon, K.F., Kiefert, L., McTainsh, G.H., 1988. Organic matter content of rural dusts in Australia. Atmos. Environ. 32, 2817–2823.
Bradford, J.M., Huang, L., 1993. Comparison of inter-rill soil loss for laboratory and field procedures. Soil Technol. 6, 145–156.
Bradford, J.M., Remley, P.A., Ferris, J.E., Santini, J.B., 1986. Effect of soil surface sealing on splash from a single waterdrop. Soil Sci. Soc. Am. J. 50, 1547–1552.
Brasington, J., Smart, R.M.A., 2003. Close-range digital photogrammetric analysis of experimental drainage basin evolution. Earth Surf. Process. Landf. 28, 231–247.
Cammeraat, L.H., 2002. A review of two strongly contrasting geomorphological systems within the context of scale. Earth Surf. Process. Landf. 27, 1201–1222.
Carmi, G., Berliner, P., 2008. The effect of soil crust on the generation of runoff on small plots in an arid environment. Catena 74, 37–42.
Casenave, A., Valentin, C., 1992. A runoff capability classification system based on surface features criteria in semi-arid areas of West Africa. J. Hydrol. 130, 231–249.
Chappell, A., Zobeck, T.M., Brunner, G., 2006. Using bi-directional soil spectral reflectance to model soil surface changes induced by rainfall and wind-tunnel abrasion. Remote Sens. Environ. 102, 328–343.
Christiansen, J.E. 1942. Irrigation by sprinkling. California Agriculture Experiment Station Bulletin, No. 670.
Connolly, R.D., Schirmer, J., Dunn, P.K., 1998. A daily rainfall disaggregation model. Agric. For. Meteorol. 92, 105–117.
Corwin, D.L., Hopmans, J., de Rooij, G.H., 2006. From field- to landscape-scale vadose zone processes: scale issues, modelling and monitoring. Vadose Zone J. 5, 129–139.
Croft, H., Anderson, K., Kuhn, N.J., 2009. Characterizing soil surface roughness using a combined structural and spectral approach. Eur. J. Soil Sci. 60, 431–442. http://dx.doi.org/10.1111/j.1365-2389.2009.01129.x.
Croft, H., Anderson, K., Brazier, R.E., Kuhn, N.J., 2013. Modeling fine-scale soil surface structure using geostatistics. Water Resour. Res. 49, 1858–1870. http://dx.doi.org/10.1002/wrer.20172.
Currence, H.D., Lovely, W.G., 1970. The analysis of soil surface roughness. Trans. ASAE 13, 710–714.
Darboux, F., Davy, Ph., Gascuel-Odoux, C., Huang, C., 2001. Evolution of soil surface roughness and flowpath connectivity in overland flow experiments. Catena 46, 125–139.
Decagon Devices Inc., 2007. Mini Disk Infiltrometer: Use Manual Version 6. Decagon Devices Inc., Pullman, WA.
Dunkerley, D., 2004. Flow threads in surface run-off: implications for the assessment of flow properties and friction coefficients in soil erosion and hydraulics investigations. Earth Surf. Process. Landf. 29, 1011–1026.
Emerson, W., Greenland, D., 1990. Soil aggregates – formation and stability. In: De Boodt, M., Hayes, M., Herbillon, A. (Eds.), Soil Colloids and Their Associations in Aggregates. Plenum Press, New York, pp. 485–511.
Esteves, M., Planchon, O., Lapetite, J.M., Silvera, N., Cadet, P., 2000. The "EMIRE" large rainfall simulator: design and field testing. Earth Surf. Process. Landf. 25, 681–690.
Evans, D.D., Buol, S.W., 1968. Micromorphological study of soil crusts. Soil Sci. Soc. Am. Proc. 32, 19–22.
Fan, Y., Lei, T., Shainberg, I., Cai, Q., 2008. Wetting rate and rain depth effects on crust strength and micromorphology. Soil Sci. Soc. Am. J. 72, 1604–1610.
FAO, 1980. Metodología provisional para la evaluación de la degradación de los suelos. Roma-Italia. (86 pp).
Farres, P., 1978. The role of time and aggregate size in the crusting process. Earth Surf. Process. 3, 243–254.
Feng, G.L., Sharratt, B., Vaddella, V., 2013. Windblown soil crust formation under light rainfall in a semiarid region. Soil Tillage Res. 128, 91–96.
Freebairn, D.M., Gupta, S.C., Rawls, W.J., 1991. Influence of aggregate size and microrelief on development of surface soil crusts. Soil Sci. Soc. Am. J. 55, 188–195.
Fu, Y., Li, G., Zheng, T., Li, B., Zhang, T., 2017. Splash detachment and transport of loess aggregate fragments by raindrop action. Catena 150, 154–160.

Furbish, D.J., Hamner, K.K., Schmeeckle, M., Borosund, M.N., Mudd, S.M., 2007. Rain splash of dry sand revealed by high-speed imaging and sticky paper splash targets. J. Geophys. Res. 112, F01001. http://dx.doi.org/10.1029/2006JF000498.
Garcia Moreno, R., Diaz Alvarez, M.C., Saa Requejo, A., Valencia Delfa, J.L., Tarquis, A.M., 2010. Multiscaling analysis of soil roughness variability. Geoderma 160, 22–30.
Ghadiri, H., Hussein, J., Rose, C.W., 2007. A study of the interactions between salinity, soil erosion, and pollutant transport on three Queensland soils. Aust. J. Soil Res. 45, 404–413.
Greene, R.S.B., Joeckel, R.M., Mason, J.A., 2006. Dry saline lakebeds as potential source areas of aeolian dust: studies from the Central Great Plains of the USA and SE Australia. In: Fitzpatrick, R.W., Shand, P. (Eds.), Regolith 2006: Consolidation and Dispersion of Ideas. CRC LEME, Perth, Australia, pp. 113–117.
Greene, R.S.B., Cattle, S.R., McPherson, A.A., 2009. Role of eolian dust deposits in landscape development and soil degradation in southeastern Australia. Aust. J. Earth Sci. 56, 55–65. http://dx.doi.org/10.1080/08120090092871101.
Helming, K., Romkens, M.J.M., Prasad, S.N., 1998. Surface roughness related processes of runoff and soil loss: a flume study. Soil Sci. Soc. Am. J. 62, 243–250.
Hu, Z., Liu, L.-Y., Li, S.-J., Cai, Q.-G., Lü, Y.-L., Guo, J.-R., 2012. Development of soil crusts under simulated rainfall and crust formation on a loess soil as influenced by polyacrylamide. Pedosphere 22, 415–424.
Huang, C., Bradford, J.M., 1990. Portable laser scanner for measuring soil surface roughness. Soil Sci. Soc. Am. J. 54, 1402–1406.
Huang, C., Bradford, J.M., 1992. Applications of a laser scanner to quantify soil microtopography. Soil Sci. Soc. Am. J. 56, 14–21.
Iserloh, T., et al., 2013. European small portable rainfall simulators; a comparison of rainfall characteristics. Catena 110, 100–112.
Jester, W., Klik, A., 2005. Soil surface roughness measurement – methods, applicability and surface representation. Catena 64, 174–192.
Kamphorst, E.C., Jetten, V., Guérif, J., Pitkänen, J., Iversen, B.V., Douglas, J.R., Paz, A., 2000. Predicting depressional storage from soil surface roughness. Soil Sci. Soc. Am. J. 64, 1749–1758.
Kidron, G.J., 2007. Millimeter-scale microrelief affecting runoff yield over microbiotic crust in the Negev Desert. Catena 70, 266–273.
Kirkby, M., 2002. Modeling the interactions between soil surface properties and water erosion. Catena 46, 89–102.
Kuipers, J., 1957. A relief meter for soil cumulative studies. Neth. J. Agric. Sci. 5, 255–262.
Kyei-Baffour, N., Rycroft, D.W., Tanton, T.W., 2004. The impacts of sodicity on soil strength. Irrig. Drain. 53, 77–85.
Le Bissonais, Y., 1996a. Aggregates stability and assessment of soil crustability and erodibility: I. Theory and methodology. Eur. J. Soil Sci. 47, 425–437.
Le Bissonais, Y., 1996b. Soil characteristics and aggregate stability. In: Agassi, M. (Ed.), Soil Erosion, Conservation and Rehabilitation. Dekker, NY, pp. 41–60.
Le Bissonais, Y., Bruand, A., Jamagne, M., 1989. Laboratory experimental study of soil crusting: relationships between aggregate breakdown mechanisms and crust structure. Catena 16, 377–392.
Leguédois, S., Planchon, O., Legout, C., Le Bissonnais, Y., 2005. Splash projection distance for aggregated soils: theory and experiment. Soil Sci. Soc. Am. J. 69, 30–37. http://dx.doi.org/10.2136/sssaj2005.0030.
Levy, G.J., Levin, J., Shainberg, I., 1994. Seal formation and interrill soil erosion. Soil Sci. Soc. Am. J. 58, 203–209.
Loch, R.J., Robotham, B.G., Zeller, L., Masterman, N., Orange, D.N., Bridge, B.J., Sheridan, G., Bourke, J.J., 2001. A multi-purpose rainfall simulator for field infiltration and erosion studies. Aust. J. Soil Res. 39, 599–610.
Long, E.J., Hargrave, G., Cooper, J.R., Kitchener, B.G.B., Parsons, A.J., Hewett, C.J.M., Wainwright, J., 2014. Experimental investigation into the impact of a liquid droplet onto a granular bed using 3D, time-resolved, particle tracking. Phys. Rev. E 89 (3). http://dx.doi.org/10.1103/PhysRevE.89.032201.
Mason, J.A., Jacobs, P.M., Greene, R.S.B., Nettleton, W.D., 2003. Sedimentary aggregates in the Peoria Loess of Nebraska, USA. Catena 53, 377–397.
Mason, J.A., Greene, R.S.B., Joeckel, R.M., 2011. Laser diffraction analysis of the disintegration of Aeolian sedimentary aggregates in water. Catena 87, 107–118.
Moncada, M.P., Gabriels, D., Lobo, D., De Beuf, K., Figueroa, R., Cornelis, W.M., 2014. A comparison of methods to assess susceptibility to soil sealing. Geoderma 226–227, 397–404.
Morin, J., Karen, R., Benjamini, Y., Ben-Hur, M., Shainberg, I., 1989. Water infiltration as affected by soil crust and moisture profile. Soil Sci. 148, 53–59.
Nciizah, A.D., Wakindiki, I.I.C., 2014. Rainfall pattern effects on crusting, infiltration and erodibility in some South African soils with various texture and mineralogy. Water SA 40, 57–64.
Nciizah, A.D., Wakindiki, I.I.C., 2015. Soil sealing and crusting effects on infiltration rate: a critical review of shortfalls in prediction models and solutions. Arch. Agron. Soil Sci. 61, 1211–1230.
Onstad, C.S., 1984. Depressional storage on tilled surfaces. Trans. ASAE 27, 729–732.
Rajot, J.L., Alfaro, S.C., Gomes, L., Gaudichet, A., 2003. Soil crusting on sandy soils and its influence on wind erosion. Catena 53, 1–16.
Ramos, M.C., Nacci, S., Pla, I., 2003. Effect of raindrop impact and its relationship with aggregate stability to different disaggregation forces. Catena 53, 365–376.
Rawlins, B.G., Wragg, J., Lark, R.M., 2013. Application of a novel method for soil aggregate stability measurement by laser granulometry with sonication. Eur. J. Soil Sci. 64, 92–103.
Rayment, G.E., Higginson, F.R., 1992. Australian Laboratory Handbook of Soil and Water Chemical Methods. Inkata Press, Pty Ltd.
Rodríguez-Caballero, E., Cantón, Y., Chamizo, S., Afana, A., Solé-Benet, A., 2012. Effects of biological soil crusts on surface roughness and implications for runoff and erosion. Geomorphology 145–6, 81–98. http://dx.doi.org/10.1016/j.geomorph.2011.12.042.
Römkens, M.J., Wang, J.Y., 1986. Effect of tillage on surface-roughness. Trans. ASAE 29, 429–433. http://dx.doi.org/10.13031/2013.30167.
Römkens, M.J.M., Helming, K., Prasad, S.M., 2001. Soil erosion under different rainfall intensities, surface roughness and soil water regimes. Catena 46, 103–123.
Rosewell, C.J., 1986. Rainfall kinetic energy in eastern Australia. J. Clim. Appl. Meteorol. 25, 1695–1701.
Ryżak, M., Bieganowski, A., Polakowski, C., 2015. Effect of soil moisture content on the splash phenomenon reproducibility. PLoS One 10 (3), e0119269. http://dx.doi.org/10.1371/journal.pone.0119269.
Salles, C., Poesen, J., Govers, G., 2000. Statistical and physical analysis of soil detachment by raindrop impact: rain erosivity indices and threshold energy. Water Resour. Res. 36, 2721–2729.
Scherer, G.W., 1990. Theory of drying. J. Am. Ceram. Soc. 73, 3–14.
Shainberg, I., 1992. Chemical and mineralogical components of crusting. In: Sumner, M.E., Stewart, B.A. (Eds.), Soil Crusting: Chemical and Physical Processes. Lewis Publishers, Boca Raton, Florida, pp. 33–53.
Shainberg, I., Letey, J., 1984. Response of soils to sodic and saline conditions. Hilgardia 52, 1–57.
Smith, M.W., 2014. Roughness in the earth sciences. Earth Sci. Rev. 136, 202–225.
Smith, M.W., Cox, N.J., Bracken, L.J., 2011. Modeling depth distributions of overland flows. Geomorphology 125, 402–413.
Sun, Y., Lin, J., Schulzelammers, P., Damerow, L., Hueging, H., Zhang, H., Sun, W., 2009. Predicting surface porosity using a fine-scale index of roughness in a cultivated field. Soil Tillage Res. 103, 57–64.
Truman, C.C., Strickland, T.C., Potter, T.L., Franklin, D.H., Bosch, D.D., Bednarz, C.W., 2007. Variable rainfall intensity and tillage effects on runoff, sediment, and carbon losses from a loamy sand under simulated rainfall. J. Environ. Qual. 36, 1495–1502.
Valentin, C., Bresson, L.M., 1992. Morphology, genesis and classification of surface crusts in loamy and sandy soils. Geoderma 55, 225–245.
Vermang, J., Norton, L.D., Baetens, J.M., Huang, C., Cornelis, W.M., 2013. Quantification of soil surface roughness evolution under simulated rainfall. Trans. ASABE 56 (2), 505–514.
Vermang, J., Norton, L.D., Huang, C., Cornelis, W.M., da Silva, A.M., Gabriels, D., 2015a. Characterization of soil surface roughness effects on runoff and soil erosion rates under simulated rainfall. Soil Sci. Soc. Am. J. http://dx.doi.org/10.2136/sssaj2014.08.0329.
Vermang, J., da Silva, A.M., Huang, C.-H., Gabriels, D., Cornelis, W.M., Norton, D., 2015b. Surface roughness effects on runoff and soil erosion rates under simulated roughness effects on runoff and soil erosion rates under simulated rainfall. Soil Sci. Soc. Am. J. http://dx.doi.org/10.2136/sssaj2014.08.0329.
Vidal Vázquez, E., Miranda, J.G.V., Paz González, A., 2006. Effect of tillage on fractal indices describing sol surface microrelief of a Brazilian Alfisol. Geoderma 134, 428–439.
Zhang, Q., Gao, M., Zhao, R., Cheng, X., 2015. Scaling of liquid-drop impact craters in wet granular media. Phys. Rev. E 92, 042205.
Zobeck, T.M., Popham, T.W., 1997. Modification of the wind erosion roughness index by rainfall. Soil Tillage Res. 42, 47–61.